

Signal Set Design with Constrained Amplitude Spectrum and Specified Time-Bandwidth Product

Girish Chandran and Jules S. Jaffe

Abstract—A new method for designing signals with a given time-bandwidth product, such that all the signals in the set have a flat amplitude spectrum and have low cross-correlation function values is introduced. It is shown that these signals lie on a signal parameter space ellipse. For a given duration and bandwidth, it is possible to trade off the cardinality of the set for better cross-correlation properties between remaining members of the set. Proof that the cross-correlation between these signals is bounded from above by a factor proportional to the square-root of inverse distance between these signals along one of the axes of the ellipse is given. It is also shown that the cross-correlation between two signals that are furthest apart is bounded by the square-root of inverse time-bandwidth product of the signals in the set. An example design is then given and a comparison of this signal set to some well-known signal sets illustrates that it performs better when the metric is maximum cross-correlation value. The proposed signal set also has the advantage that it can be designed for any time-bandwidth product instead of discrete values.

I. INTRODUCTION

CONSIDERABLE effort has been devoted to the problem of synthesizing signal sets that have low values of cross-correlation at all lags and low values of auto-correlation at nonzero lags [1]–[5]. The need for such signal sets arise in many applications. One such application is a code division multiple access communication system that provides multiple users with signals that utilize the full bandwidth of the channel. Such a system requires a large number of signals in the set and for unambiguously separating the different signals, low values of cross-correlation. This work evolved out of trying to design signals for a multibeam imaging scheme that transmits multiple signals for fast imaging rates [6], [7]. There is no attempt to have a large family of signals. In fact, when examining existing signal sets for this application, it seemed that there must be a way to trade off large family sizes of popular signal sets for smaller values of cross-correlation between members of the set. An additional criterion signal set design is for all the signals to use all the available system bandwidth. In this application, detection of discrete targets in the image and the ability to estimate target parameters are important.

Paper approved by S. Benedetto, the Editor for Signal Design, Modulation, and Detection of the IEEE Communications Society. Manuscript received December 19, 1994; revised June 27, 1995. This work was supported by the National Science Foundation under Grants OCE 89-14300 and OCE 9421876. This paper was presented in part at the International Symposium on Information Theory, Whistler, BC, Canada, September 1995.

G. Chandran is with the Department of Electrical Engineering, University of California, San Diego, CA 92093 USA.

J. S. Jaffe is with the Marine Physical Laboratory, Scripps Institution of Oceanography, La Jolla, CA 92093 USA.

Publisher Item Identifier S 0090-6778(96)04349-8.

For target detection, there is often a requirement to maximize the signal-to-noise ratio (SNR) at the output of the receiver. Both Bayes and Neyman–Pearson strategies to optimize the probability of target detection maximize the SNR at the output of the receiver [8], [9]. To maximize the SNR at the output of the receiver, a receive filter with the inverse backscattering spectrum can be used. An alternative design philosophy is to have the transmitted signal be the inverse backscattering spectrum [10]. SNR at the output of a receiver can be raised by an appropriate choice of signals. Using a narrow band signal could cause severe time-varying fading when the transmitted signal, reflecting from various parts of the target destructively interfere with each other. Using a signal whose spectrum is broad enough to cover nulls in the backscattering spectrum will ensure that there is reasonable SNR at the input to the receiver, even when some frequencies are attenuated.

Let the Fourier transform of unit energy signals s_i be defined as $S_i(f) = \int_{-\infty}^{+\infty} s_i(t)e^{-j2\pi ft} dt$. For $i = 1, 2, \dots, N$ let

$$\frac{\int_{-W}^W |S_i(f)|^2 df}{\int_{-\infty}^{+\infty} |S_i(f)|^2 df} \geq 1 - \epsilon.$$

The fraction of energy outside the band of interest $[-W, W]$ (determined by the backscattering spectrum), is bounded by ϵ , $0 < \epsilon < 1$. The signal that maximizes the SNR at the receiver output is an eigenfunction corresponding to the maximum eigenvalue of the Fredholm integral equation

$$\lambda_i s_i(t) = \int_{-\frac{T}{2}}^{\frac{T}{2}} s_i(t) 2W \frac{\sin 2\pi W(t - \tau)}{2\pi W(t - \tau)} d\tau$$

where T is the duration of the signals. In fact, the signal set $S = \{s_1(t), s_2(t), \dots\}$ consisting of eigenfunctions corresponding to the ordered sequence of eigenvalues $\lambda_1 \geq \lambda_2 \geq \lambda_3 \geq \dots$ is the set of angular prolate spheroidal wave functions [10]–[14]. Of these, the first $2WT$ signals have significant energy in $[-\frac{T}{2}, \frac{T}{2}] \times [-W, W]$ and will give SNR's that are large and comparable. Although these signals are orthogonal, the cross-correlation between the signals is not zero for all lags.

In this work, a systematic design procedure for designing signals with a given time-bandwidth product (both time and bandwidth are independently specified) such that they satisfy a flat spectral amplitude constraint and have low cross-correlation values is introduced. Section II introduces the conditions that are to be satisfied by all the members of

the signal set and shows that the shape of the ideal cross-correlation function should be a constant function over the support. Since the amplitudes of the signal Fourier transforms are constrained to be flat, only the phase of the transform can be specified to satisfy the other constraint. The reason for the choice of a quadratic phase structure for the Fourier transforms of the signals is discussed in Section III. It is shown that the quadratic coefficients are constrained to lie on an ellipse in the signal parameter space, by the choice of the duration and bandwidth of the signal set. It is shown that the cross-correlation between signals varies as the square-root of the inverse distance between signals along one axis of the ellipse. Proof that the cross-correlation between two signals that are furthest apart in the set varies as the square-root of the inverse time-bandwidth product of the signals in the set is given. The results of a design using the method is then presented in Section V. The trade-off involved between the number of elements of the signal set and the cross-correlation between signals in the set is made clear using an example. Finally, a comparison of the new design with some older ones is made.

II. SIGNAL SET DESIGN SPECIFICATIONS

A. Constraints Imposed on the Signal Set

The properties that characterize the signals belonging to the set are outlined below. All the signals belonging to the set should have the same energy. Without loss of generality, it can be assumed that all the signals have unit energy. For the receiver to distinguish between signals, another condition is needed. The cross-correlation between signals is required to be small. The correlation conditions have been used in designing other signal sets [3]. Finally, all the signals in the set are constrained to have the same flat amplitude spectrum. To state these constraints mathematically, design a set of signals given by the set $\mathbf{S} = \{s_1(t), s_2(t), \dots, s_N(t)\}$ that are $L_2(\frac{-T}{2}, \frac{T}{2})$ with a corresponding set of Fourier transforms $\mathcal{S} = \{\mathcal{S}_1(f), \mathcal{S}_2(f), \dots, \mathcal{S}_N(f)\}$ satisfying the following conditions.

Condition 1:

$$\int_{-\frac{T}{2}}^{\frac{T}{2}} |s_i(t)|^2 dt = 1; \quad i = 1, \dots, N. \quad (1)$$

Condition 2: For some $\kappa > 0$ and for all $\tau \leq T$

$$|R_{i,j}(\tau)| < \kappa; \quad i, j = 1, \dots, N; \quad i \neq j \quad (2)$$

where the cross-correlation $R_{i,j}(\tau)$ between signals $s_i(t)$ and $s_j(t)$ is defined as

$$R_{i,j}(\tau) = \int_{-T}^{+T} s_i(t) s_j^*(t - \tau) dt; \quad \tau \leq T.$$

It will be shown later how the value of κ relates to the time-bandwidth product.

Condition 3: For $i = 1, 2, \dots, N$

$$|\mathcal{S}_i(f)| = \begin{cases} \alpha_1; & |f| \leq W, \\ \alpha_2(f); & |f| > W \end{cases} \quad (3)$$

where α_1 is a constant and $\alpha_2(f)$ is positive function such that $\int_{-\infty}^{+\infty} |\mathcal{S}_i(f)|^2 df = 1$ and $\int_{-W}^W |\mathcal{S}_i(f)|^2 df = 1 - \epsilon$, $0 < \epsilon < 1$. The signals are essentially band-limited with the amplitude of the Fourier transform as specified.

B. Shape of the Ideal Cross-Correlation Function

The cross-correlation $R_{i,j}(\tau)$ between signals $s_i(t)$ and $s_j(t)$ can also be written as

$$R_{i,j}(\tau) = \int_{-\infty}^{+\infty} \mathcal{S}_i(f) \mathcal{S}_j^*(f) e^{2\pi j f \tau} df. \quad (4)$$

It follows from (3), (4), and Plancherel's relation that

$$\int_{-T}^{+T} |R_{i,j}(\tau)|^2 d\tau = \int_{-\infty}^{+\infty} |\mathcal{S}_i(f)|^4 df = \int_{-T}^{+T} |R_{i,i}(\tau)|^2 d\tau.$$

Since $s_i(t)$'s are unit energy signals (Condition 1), $|R_{i,j}(\tau)|^2$ is a bounded continuous function on a bounded interval $[-T, T]$. $\int_{-T}^{+T} |R_{i,j}(\tau)|^2 d\tau$ is, therefore, finite. Hence, so is $\int_{-\infty}^{+\infty} |\mathcal{S}_i(f)|^4 df$. The equality shows that the area under the squared magnitude of the both cross and auto-correlation functions is a constant. Since uniformly low cross-correlation values is of primary interest, it can be reasoned from the equation as to what the shape of the ideal cross-correlation function should be. It should be a constant function with a support $[-T, T]$ to achieve the uniformly lowest values possible. Any other shape for the function will have some values which are larger than that obtained for the constant function.

III. PHASE FUNCTION IN THE FREQUENCY DOMAIN

It can be shown that the functional form or the shape of the complex envelopes of the signal in both the frequency and time domains will be approximately rectangular if the phase functions for the signal in the time and frequency domains are quadratic [15]. This provides a starting point. Functions with nonlinear phase structure in the time domain are usually termed pulse compression signals in radar and sonar literature. One type of pulse compression signal is the linear frequency modulated (FM) signal. Linear FM signals or chirps were first studied more than three decades ago. These signals have a quadratic phase structure in the time domain. It has been shown that the amplitude of the Fourier transform of the chirp signals can be made reasonably flat with a large time-bandwidth product [16]. By duality of Fourier transform, it follows that if the Fourier transform of a signal has a constant amplitude and quadratic phase structure, then the signal itself will have a complex envelope whose amplitude is reasonably flat for large time-bandwidth products.

From (4) and the discussion above, the strategy for the design of signals is clear. Choose signals that have a constant amplitude and quadratic phase structure in the frequency domain. The product of the Fourier transform of one signal

and the complex conjugate of the Fourier transform of another will still be a constant amplitude function. The phase function of the product of Fourier transforms will be the difference between the two quadratic phase functions of the individual signal Fourier transforms. Since the difference function also has to have a quadratic phase, quadratic coefficients for the individual signals is chosen appropriately. Let

$$s_i(t) = \mu_i(t)e^{j\phi_i(t)} \quad (5)$$

and let the Fourier transform of $s_i(t)$, $S_i(f)$ be given by

$$S_i(f) = |S_i(f)|e^{j\theta_i(f)} \quad (6)$$

where the phase of signal $S_i(f)$ is

$$\theta_i(f) = a_i f^2 + b_i f + c_i. \quad (7)$$

However, from (7) it is not clear how to pick the values for a_i , b_i , and c_i for the signals.

A. Dependence of the Quadratic Coefficients on the Duration and Bandwidth of the Signals

Since the duration and bandwidth of the signals are fixed and known, it seems unreasonable that the quadratic coefficients can be chosen arbitrarily. In fact, there is a relation between the duration, bandwidth and the quadratic coefficients. To arrive at the rule to pick these quadratic coefficients, some additional definitions are needed.

Assume that all the signals in the signal set have the same root mean square (rms) duration γ and rms bandwidth β , where using the usual definitions

$$\gamma^2 = (2\pi)^2 \int_{-\infty}^{+\infty} t^2 |s_i(t)|^2 dt \quad (8)$$

$$\beta^2 = (2\pi)^2 \int_{-\infty}^{+\infty} f^2 |S_i(f)|^2 df \quad (9)$$

where $s_i(t)$ and $S_i(f)$ are from (5) and (6). In other words, for signals with unit energy, the rms duration is the square root of the second moment of the magnitude of the complex envelope of the signal in the time domain and the rms bandwidth is the square root of the second moment of the complex envelope of the magnitude of the signal in the frequency domain. Rms duration γ can be expressed in terms of the frequency domain parameters and rms bandwidth β can be expressed in terms of the time domain parameters as follows [15]:

$$\gamma^2 = \int_{-\infty}^{+\infty} |S'_i(f)|^2 df \quad (10)$$

$$\beta^2 = \int_{-\infty}^{+\infty} |s'_i(t)|^2 dt. \quad (11)$$

Using the above definitions, it can be shown without difficulty (Appendix A) that the equation governing the relationship between the quadratic coefficients and the rms duration and rms bandwidth is

$$\frac{a_i^2}{\left(\frac{\pi\gamma}{\beta}\right)^2} + \frac{b_i^2}{\gamma^2} = 1. \quad (12)$$

In terms of the duration T and bandwidth $2W$

$$\frac{a_i^2}{\left(\frac{\pi T}{2W}\right)^2} + \frac{b_i^2}{\frac{\pi T}{3}} = 1. \quad (13)$$

Given the signal duration and the signal bandwidth, it can be seen from (12) and (13) above that the quadratic coefficients a_i and b_i lie along an ellipse. Each point on the ellipse, (a_i, b_i) , represents a quadratic phase function $\theta_i(f)$ and, thus, a signal $s_i(t)$. The semi-minor axis has a length $2\frac{\pi T}{2W}$ and the semi-major axis has a length $2\frac{\pi T}{\sqrt{3}}$. Thus, for different durations and different bandwidths, there are different signal ellipses.

B. An Upper Bound for the Maximum Cross-Correlation

The cross-correlation function can now be examined. Substituting (A1), (6) and (7) in (4)

$$R_{i,j}(\tau) = \int_{-W}^{+W} \left(\frac{1}{\sqrt{2W}} - \delta_1 \right)^2 \cdot e^{j(\Delta a f^2 + \Delta b f + \Delta c)} e^{2\pi j f \tau} df + O(\delta_2) \quad (14)$$

where

$$\Delta a = a_i - a_j; \quad \Delta b = b_i - b_j; \quad \Delta c = c_i - c_j$$

and $2W$ is the bandwidth of the signals. This expression can be simplified to

$$R_{i,j}(\tau) = \int_{-W}^{+W} \frac{1}{2W} e^{j(\Delta a f^2 + \Delta b f + \Delta c)} \cdot e^{2\pi j f \tau} df + O(\max(\delta_1, \delta_2)). \quad (15)$$

To simplify notation, $O(\max(\delta_1, \delta_2))$ will, henceforth, be omitted in equations involving $R_{i,j}(\tau)$. Restating (15)

$$R_{i,j}(\tau) = \int_{-W}^{+W} \frac{1}{2W} e^{j(\Delta a f^2 + \Delta b f + \Delta c)} e^{2\pi j f \tau} df.$$

Rewriting this equation as

$$R_{i,j}(\tau) = e^{j\Delta c} \int_{-W}^{+W} \frac{1}{2W} e^{j\Delta a f^2} e^{2\pi j f(\tau + \frac{\Delta b}{2\pi})} df \quad (16)$$

it can be seen that the coefficient Δb represents a time shift and the coefficient Δc a phase shift in $R_{i,j}(\tau)$. The shape of the cross-correlation envelope is thus controlled by the choice of the quadratic coefficient Δa . Since we require the shape of the cross-correlation function to be as flat as possible (Section II-B), we must choose Δa appropriately. It is also of interest to see what the maximum value of $|R_{i,j}(\tau)|$ will be and how it relates to Δa . To investigate that, an additional result is required.

Lemma (Continuity): $R_{i,j}$ is a continuous function of τ , Δa , Δb , and Δc .

Proof: Let

$$g(f, \tau, \Delta a, \Delta b, \Delta c) = e^{j(\Delta a f^2 + (\Delta b + 2\pi\tau)f + \Delta c)}.$$

Then $R_{i,j}(\tau, \Delta a, \Delta b, \Delta c) = \int_{-W}^{+W} g df$. g is continuous in f , τ , Δa , Δb , Δc . For a fixed Δa , Δb , Δc , clearly $g(\cdot, \tau, \Delta a, \Delta b, \Delta c): [-W, +W] \rightarrow \mathbf{C}$ is continuous and, therefore, integrable for each $\tau \in [-\frac{T}{2}, \frac{T}{2}]$ (\mathbf{C} is the set of complex numbers). Since g is continuous on the closed and bounded interval $[-W, W]$, g attains a maximum value, say $M(\tau)$ on $[-W, +W]$. $|g(f, \tau, \cdot, \cdot, \cdot)| \leq M(\tau)$ for all f , τ . Applying the dominated convergence theorem to the sequence of functions $g_n(f) = g(f, \tau_n)$, it follows that $R_{i,j}$ is continuous in τ . Proof for Δa , Δb , Δc is similar. \square

Since $R_{i,j}(\tau)$ is a continuous function, so is $|R_{i,j}(\tau)|$. This means that $\max_{\tau \leq T} |R_{i,j}(\tau)|$ exists and is finite.

$$\text{Theorem: } \max_{|\tau| \leq T} |R_{i,j}(\tau)| \leq 2.3 \left(\frac{1}{2W} \sqrt{\frac{\pi}{2\Delta a}} \right)$$

Proof: Evaluating the inverse Fourier transform of (15) (Appendix B)

$$R_{i,j}(\tau) = \frac{1}{2W} \sqrt{\frac{\pi}{2\Delta a}} [C(x_1) + jS(x_1) - C(x_0) - jS(x_0)] \cdot \exp \left\{ -j \left[\frac{(2\pi\tau + \Delta b)^2}{\Delta a} - \Delta c \right] \right\} \quad (17)$$

where

$$C(x) = \int_0^x \cos \left(\frac{\pi t^2}{2} \right) dt$$

and

$$S(x) = \int_0^x \sin \left(\frac{\pi t^2}{2} \right) dt$$

are the real and imaginary parts of a Fresnel integral and $x_1 = \sqrt{\frac{2}{\pi\Delta a}}((2\pi\tau + \Delta b) + W\Delta a)$ and $x_0 = \sqrt{\frac{2}{\pi\Delta a}}((2\pi\tau + \Delta b) - W\Delta a)$

$$|R_{i,j}(\tau)| = \frac{1}{2W} \sqrt{\frac{\pi}{2\Delta a}} |C(x_1) + jS(x_1) - C(x_0) - jS(x_0)|. \quad (18)$$

$\max_{x_0, x_1 \in (-\infty, +\infty)} [|C(x_1) - C(x_0)|] \leq 1.6$. Also, $\max_{x_0, x_1 \in (-\infty, +\infty)} [|S(x_1) - S(x_0)|] \leq 1.6$. Thus

$$|C(x_1) + jS(x_1) - C(x_0) - jS(x_0)| \leq 2.3. \quad \square$$

Since τ appears only in the limits of the function $C(x) + jS(x)$, the shape of $|R_{i,j}(\tau)|$ is controlled by the function $|C(x) + jS(x)|$ for a given Δa and Δb . Define $\kappa = 2.3 \left(\frac{1}{2W} \sqrt{\frac{\pi}{2\Delta a}} \right)$. Then condition (2) is satisfied. The theorem implies that $\max_{\tau \leq T} |R_{i,j}(\tau)|$ varies as $\frac{1}{\sqrt{\Delta a}}$. The dependence of this bound on the duration is through the term Δa , which also depends on the bandwidth.

Corollary: For a given duration and bandwidth for the signal set, the modulus of the cross-correlation between two signals that are furthest apart along the semi-minor axis, in the set is bounded above by $\frac{1}{\sqrt{TW}}$.

Proof: For a given time-bandwidth product, the maximum separation between signals along the a_i axis between any two signals is between the ones at the end points of the ellipse. For these two values of a_i , b_i is zero. Using (13), $a_i = \frac{\pi T}{2W}$. Thus, $\Delta a = \frac{2\pi T}{2W}$. From the Theorem

$$\max_{|\tau| \leq T} |R_{i,j}(\tau)| \leq \sqrt{\frac{1}{TW}}.$$

IV. DESIGN OF CONSTANT TIME-BANDWIDTH PRODUCT SIGNAL SET WITH UNIFORM CROSS-CORRELATION VALUES

As an example, the design of a signal set with all the signals having a bandwidth of 30 kHz and duration of 1 ms is illustrated here. This choice of the duration and bandwidth was appropriate for a multibeam sonar imaging system that transmits multiple signals simultaneously for fast imaging rates. The time-bandwidth product of the system is then 30. The signal ellipse corresponding to this duration and bandwidth product is chosen (Fig. 1). Starting with two signals $s_1(t)$ and $s_2(t)$, (a_1, b_1) and (a_2, b_2) are picked as shown in Fig. 1. $\Delta a (= a_1 - a_2)$ and $\Delta b (= b_1 - b_2)$ to be used in (16) are now available. Fig. 2 shows the cross-correlation magnitude between $s_1(t)$ and $s_2(t)$. Note that the cross-correlation magnitude is spread out over the support $[-T, T]$. Now, another signal $s_3(t)$ is introduced into the set. Fig. 3 shows the cross-correlation magnitude between s_1 and s_3 [and also s_3 and s_2 by (16)]. It is clear that $\max_{\tau} |R_{1,2}(\tau)| < \max_{\tau} |R_{1,3}(\tau)|$ and $\max_{\tau} |R_{2,3}(\tau)|$. A fourth signal $s_4(t)$ is introduced into the set, and $R_{1,4}(\tau)$ is computed (Fig. 4). It is seen that $\max_{\tau} |R_{1,2}(\tau)| < \max_{\tau} |R_{1,4}(\tau)|$ and also $R_{1,4}(\tau)$ looks like $R_{1,1}(\tau)$, the auto-correlation of $s_1(t)$. This is not surprising since it follows from the continuity (Lemma) of the cross-correlation function in (16), in Δa and Δb . Observing the behavior of $R_{i,j}(\tau)$ with respect to Δb , it can be noted that the position of the vertical line of symmetry in Figs. 2–4 has shifted away from $\tau = 0$ by an amount that is proportional to Δb [in agreement with (16)]. More important is the observation that as Δa becomes larger, $\max_{\tau} |R_{i,j}(\tau)|$ decreases and $|R_{i,j}(\tau)|$ becomes closer and closer to the ideal cross-correlation function. Not surprisingly, for a given time-bandwidth product, as the number of signals increase, the separation among them decreases and therefore, the cross-correlations between signals increase and κ in condition (2) increases.

Figure 5 shows the maximum value of the cross-correlation function between s_1 with coordinates (a_1, b_1) and other signals as the point (a_i, b_i) moves along the ellipse starting at the bottom of the ellipse at coordinates (a_2, b_2) and going to the top (a_1, b_1) along an counterclockwise direction, in equally spaced steps along the a axis. As the point (a_i, b_i) moves along, $\Delta a (= a_1 - a_i)$ reduces and the maximum value of cross-correlation increases. The figure also shows that the upper bound from the theorem (solid line) closely follows the values of maximum cross-correlation for Δa 's that are not very small. There are an infinity of a_i 's and b_i 's that can be picked from the ellipse and the values of a_i 's and b_i 's that would minimize (18) with $(\Delta a = a_i - a_j)$ and $(\Delta b = b_i - b_j)$ have to be determined. To do this, (18) can be differentiated

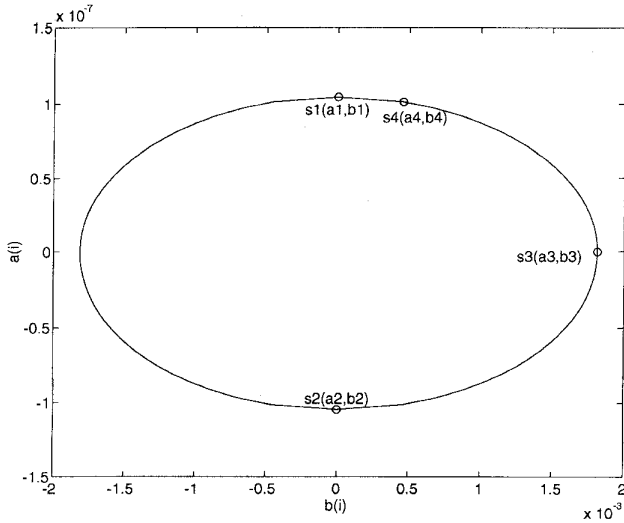


Fig. 1. The relationship between the quadratic coefficients a_i and b_i for a time-bandwidth product of 30.

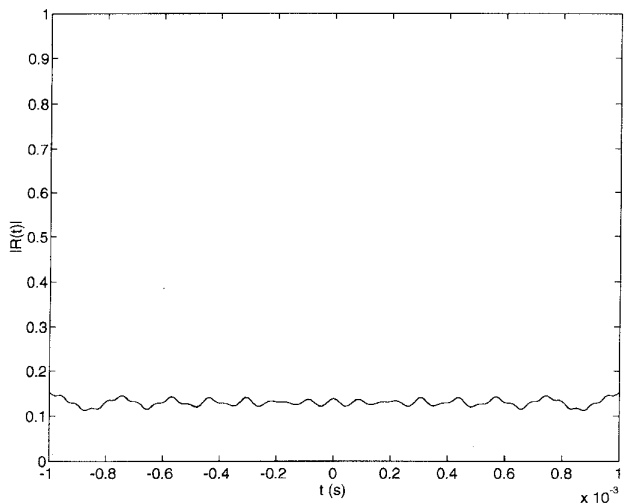


Fig. 2. Cross-correlation between s_1 and s_2 . It is nearly flat.

with respect to Δa and Δb and then the right-hand side of the equation set to zero to solve for Δa and Δb that give minimum $|R_{i,j}(\tau)|$. This method is very unwieldy. Since the maximum value of cross-correlation is not monotonic with a as can be seen from Fig. 5, there is no straightforward rule to decide which a_i 's and b_i 's to pick for an optimum (minimum values of maximum cross-correlation) signal set. In this particular case, the values of maximum cross-correlation seem to suggest a $\frac{p}{\sqrt{\Delta a}}$ type overall trend, where p is some real number. One rule that is reasonable, would be to pick signals that are as far apart along the a -axis as possible. This would suggest a linear equipartition of the axis, since any other scheme would have smaller values of Δa between signal pairs in the set and, thus, a larger figure of merit. So if there are N signals, the a_i 's for the signals are picked so that they are equally spaced along the a_i axis. Then the b_i 's corresponding to these a_i 's are chosen. Once a_i 's and b_i 's are picked, the difference between

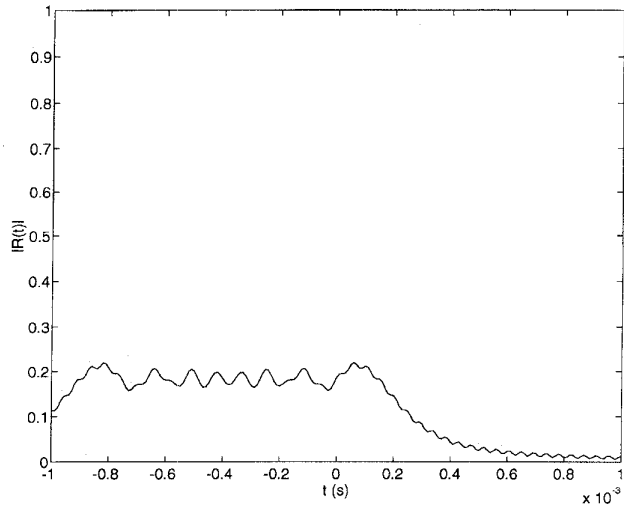


Fig. 3. Cross-correlation between s_1 and s_3 (and s_2 and s_3).

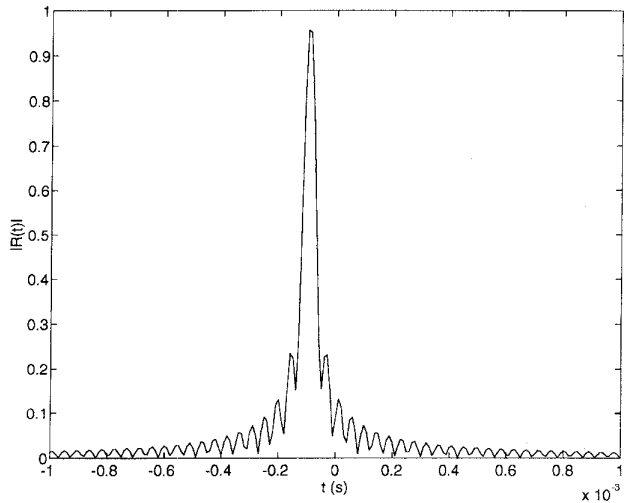


Fig. 4. Cross-correlation between s_1 and s_4 . As the signal s_j moves closer to s_1 , the cross-correlation between s_j and s_1 begins to look like the auto-correlation of s_1 .

the quadratic coefficients can be computed to arrive values for Δa and Δb . Having determined the quadratic coefficients, the cross-correlation between the chosen signals can then be computed. It is important to note that, in this scheme, the Δa distance between signal pairs reduces exponentially as $\frac{1}{2^N}$, where N is the number of signals in the set, whereas, the maximum value of the cross-correlation function between any two signals has a $\frac{p}{\sqrt{\Delta a}}$ trend.

Figure 6 shows the cross-correlation between signals in various signal sets. The maximum cross-correlation values for sequence sets shown in the figure are from the bounds given in [1]–[3]. For sequences, if bandwidth is defined as the inverse of a chip duration, then the sequence length is the same as the time-bandwidth product. With finite system bandwidths, performance of these sequences will be poorer than indicated. The line represents the cross-correlation between two linear FM signals, one sweeping up in frequency and the other sweeping

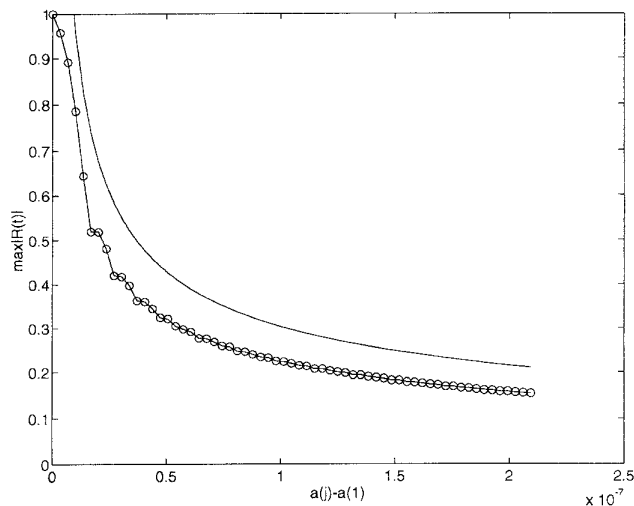


Fig. 5. Maximum value of cross-correlation between signal pairs s_1 (s_i) and s_j , for various s_j . The solid line is the upper bound from the theorem.

down in frequency. It can be shown that the maximum value of cross-correlation between the two signals varies as $\frac{1}{\sqrt{2TW}}$. It can be seen that this outperforms all the other signal sets and hints at a lower bound on the maximum cross-correlation between signals in *any* set. The disadvantage is that there are only two signals in the set. The design method elaborated here, clearly shows the trade-off between the number of signals in the set and the maximum cross-correlation between any two signals in the set. For example, if there are only two signals in the set (with a time-bandwidth product of 30), it performs almost as well as the set consisting of only two linear FM signals with the same time-bandwidth product. As a third signal is included, the maximum value of cross-correlation between the signals increases. If we use the linear equipartition rule and introduce a fourth signal, then we find from Fig. 5 that the figure of merit is about 0.25. However, this set of four signals is still better than the other sets in Fig. 6. A fifth signal would increase this figure to almost 0.3. At this point however, a subset of sequences selected from the Gold sequence set with 33 codes (a time-bandwidth product of 31) perform equally well. It is therefore possible to construct a set of signals in a systematic way, provided the number of signals required is not large with correlation properties that are better than some of the existing signal sets.

Let $\sigma = \max_N(\max_{\tau} |R_{i,j}(\tau)|)$, where N is the signal set size. The smaller σ is, better the signal set is. As is often the case, there is no need for a large family size. Instead, there is a requirement for small signal sets with as low a σ as possible. It may be possible to select a smaller subset (called optimal phases in literature [18]) of Gold sequences or Kasami sequences, for an asynchronous system. This is, however, a computationally intensive search and becomes difficult for large sequence lengths or time-bandwidth products. The design procedure outlined above has two significant advantages over selecting families of sequences. The signal set size determines σ for a given time-bandwidth product. The example showed the trade-off between

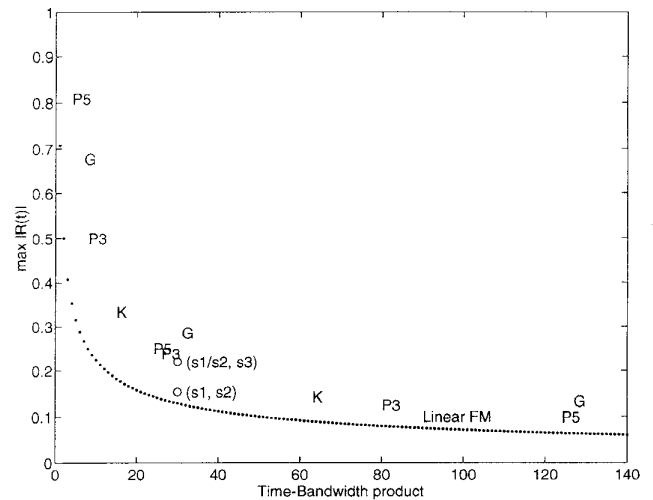


Fig. 6. Comparison of signal sets: G = Gold, K = Kasami, $P3$ = prime-phase(3), $P5$ = prime-phase(5). For these signals, the bandwidth was considered to be the inverse of the chip duration.

the number of signals and σ . This is a systematic way to arrive at the required signals, instead of searching through large families for the appropriate signals. Another advantage of this signal set over other signal sets, is that signals can be designed for all time-bandwidth products, instead of certain special ones, which is the case with sequences. This becomes clear when, for example, in trying to design signal sets with a time-bandwidth product of say, between 31 and 60 or between 81 and 120, it can be seen from Fig. 6 that there are no good sequences available. The disadvantage of this design procedure is the exponential decrease in the Δa distance between signals, as the number of signals increases.

V. SUMMARY

There are many applications where a family of signals with flat amplitude spectrum and small cross-correlation values can be used. Constraints imposed on the signals in the set were formulated in Section II. It was then reasoned out what the shape of the ideal cross-correlation function should be. It was shown this functional form can be achieved with a quadratic phase function as the Fourier transform of the signals. It was found that the coefficients cannot be arbitrarily chosen. Instead, there is a relationship between the coefficients of the quadratic phase function and the duration and bandwidth of the signals. It was shown that for a given time and bandwidth for the signals, the quadratic coefficients lie on an ellipse. The cross-correlation function was analyzed to see what the best possible values for the quadratic coefficients were. It was seen that the signals should be chosen such that the distance between them along one of the axes of the ellipse is as large as possible. Note that the values of maximum cross-correlation between different signals is different. A signal set construction procedure was outlined. An example illustrated that signals separated by the largest a distance have the least maximum cross-correlation value. This maximum is bounded by the square-root of the inverse time-bandwidth of the signals.

For a given time-bandwidth product, as the number of signals in the set increases, the separation between them decreases and the maximum value of cross-correlation between them increases. A comparison of various signal sets with respect to the maximum cross-correlation values brought out the relative merits of the signal sets. The new signal set was shown to outperform some other commonly used signal sets, as long as the number of signals required was limited. It was also indicated that new signal set also has the added advantage that it can be designed for any time-bandwidth product, unlike any of the other signal sets.

APPENDIX A

Let

$$|S_i(f)| = \begin{cases} \left(\frac{1}{\sqrt{2W}} - \delta_1\right); & |f| \leq W \\ \delta_2(f); & f > W \end{cases} \quad (\text{A1})$$

and

$$\theta_i(f) = a_i f^2 + b_i f + c_i.$$

From (10)

$$\begin{aligned} \gamma^2 &= \frac{1}{2W} \int_{-W}^W (2a_i f + b_i)^2 df + O(\delta_2) \\ &= \frac{4a_i^2 W^2}{3} + b_i^2 + O(\delta_2). \end{aligned} \quad (\text{A2})$$

Restating (9)

$$\beta^2 = (2\pi)^2 \int_{-W}^W f^2 |S_i(f)|^2 df.$$

Using (A1) in the above equation

$$\beta = \frac{2\pi W}{\sqrt{3}} + O(\delta_2). \quad (\text{A3})$$

From (A2) and (A3), neglecting $O(\delta_2^2)$, the above equation becomes

$$a_i^2 \left(\frac{\beta}{\pi}\right)^2 + b_i^2 = \gamma^2$$

which is (12).

APPENDIX B

Restating (15)

$$\begin{aligned} R_{i,j}(\tau) &= \int_{-W}^{+W} \frac{1}{2W} e^{j(\Delta a f^2 + \Delta b f + \Delta c)} \\ &\quad \cdot e^{2\pi j f \tau} df + O(\max(\delta_1, \delta_2)). \end{aligned}$$

Let $\Delta b' = \Delta b + 2\pi$. Then

$$\begin{aligned} R_{i,j}(\tau) &= \frac{1}{2W} \left\{ \int_{-W}^W \cos(\Delta a f^2 + \Delta b f + \Delta c) df \right. \\ &\quad \left. + j \int_{-W}^W \sin(\Delta a f^2 + \Delta b f + \Delta c) df \right\} \\ &\quad + O(\max(\delta_1, \delta_2)). \end{aligned}$$

Here again, we have dropped $O(\max(\delta_1, \delta_2))$ for simplicity of notation. Using (7.4.38) and (7.4.39) in [17]

$$\begin{aligned} R_{i,j}(\tau) &= \frac{1}{2W} \left\{ \sqrt{\frac{\pi}{2a}} \left[\cos\left(\frac{\Delta b'^2 - \Delta a \Delta c}{\Delta a}\right) \right. \right. \\ &\quad \cdot C\left(\sqrt{\frac{2}{\pi \Delta a}}(\Delta a f + \Delta b')\right) \\ &\quad \left. \left. + \sin\left(\frac{b'^2 - ac}{a}\right) \right. \right. \\ &\quad \left. \left. \cdot S\left(\sqrt{\frac{2}{\pi \Delta a}}(\Delta a f + \Delta b')\right) \right] \right. \\ &\quad \left. + j \sqrt{\frac{\pi}{2\Delta a}} \left[\cos\left(\frac{\Delta b'^2 - \Delta a \Delta c}{\Delta a}\right) \right. \right. \\ &\quad \cdot C\left(\sqrt{\frac{2}{\pi \Delta a}}(\Delta a f + \Delta b')\right) \\ &\quad \left. \left. - \sin\left(\frac{\Delta b'^2 - \Delta a \Delta c}{\Delta a}\right) \right. \right. \\ &\quad \left. \left. \cdot S\left(\sqrt{\frac{2}{\pi \Delta a}}(\Delta a f + \Delta b')\right) \right] \right\} \Big|_{-W}^W \end{aligned}$$

where the notation $f(x)|_{-W}^W$ implies $f(W) - f(-W)$ and $C(x) = \int_0^x \cos(\frac{\pi t^2}{2}) dt$, and $S(x) = \int_0^x \sin(\frac{\pi t^2}{2}) dt$. The equation above can be rewritten as

$$\begin{aligned} R_{i,j}(\tau) &= \frac{1}{2W} \left\{ \sqrt{\frac{\pi}{2\Delta a}} \cos\left(\frac{\Delta b'^2 - \Delta a \Delta c}{\Delta a}\right) \right. \\ &\quad \cdot \left[C\left(\sqrt{\frac{2}{\pi \Delta a}}(\Delta a f + \Delta b')\right) \right] \\ &\quad \left. + j S\left(\sqrt{\frac{2}{\pi \Delta a}}(\Delta a f + \Delta b')\right) \right. \\ &\quad \left. - j \sin\left(\frac{\Delta b'^2 - \Delta a \Delta c}{\Delta a}\right) \right. \\ &\quad \cdot C\left(\sqrt{\frac{2}{\pi \Delta a}}(\Delta a f + \Delta b')\right) \\ &\quad \left. + j S\left(\sqrt{\frac{2}{\pi \Delta a}}(\Delta a f + \Delta b')\right) \right\} \Big|_{-W}^W. \end{aligned}$$

By combining terms in the above equation

$$\begin{aligned} R_{i,j}(\tau) &= \frac{1}{2W} \sqrt{\frac{\pi}{2\Delta a}} [C(x_1) + jS(x_1) - C(x_0) - jS(x_0)] \\ &\quad \cdot \exp\left\{-j\left[\frac{(2\pi\tau + \Delta b)^2}{\Delta a} - \Delta c\right]\right\} \\ &\quad + O(\max(\delta_1, \delta_2)) \end{aligned}$$

which is (17) where

$$x_1 = \sqrt{\frac{2}{\pi \Delta a}} ((2\pi\tau + \Delta b) + W\Delta a)$$

and

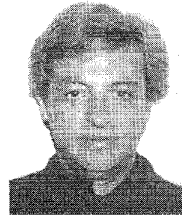
$$x_0 = \sqrt{\frac{2}{\pi \Delta a}} ((2\pi\tau + \Delta b) - W\Delta a).$$

REFERENCES

- [1] D. V. Sarwate and M. B. Pursley, "Cross-correlation properties of pseudorandom and related sequences," *Proc. IEEE*, vol. 68, no. 5, pp. 593–619, 1980.
- [2] S. Boztas, R. Hammons, and P. V. Kumar, "4-phase sequences with near-optimum correlation properties," *IEEE Trans. Inform. Theory*, vol. 38, no. 3, pp. 1101–1113, 1992.
- [3] P. V. Kumar and O. Moreno, "Prime-phase sequences with periodic correlation properties better than binary sequences," *IEEE Trans. Inform. Theory*, vol. 37, no. 3, pp. 603–616, 1991.
- [4] N. B. Chakrabarti and M. Tomlinson, "Design of sequences with specified autocorrelation and cross correlation," *IEEE Trans. Commun.*, vol. 28, no. 11, pp. 1246–1252, 1982.
- [5] J. D. Olsen, R. A. Scholtz, and L. R. Welch, "Bent-function sequences," *IEEE Trans. Inform. Theory*, vol. 28, no. 6, pp. 858–864, 1982.
- [6] J. S. Jaffe, P. M. Cassareau, and D. J. Glassbrenner, "Code design and performance characterization for code multiplexed imaging," *IEEE Trans. Acoust. Speech Signal Processing*, vol. 38, no. 8, pp. 1321–1329, 1990.
- [7] J. S. Jaffe, E. Reuss, D. McGehee, and G. Chandran, "FTV, a sonar for tracking macrozooplankton in 3-dimensions," *Deep Sea Res. I*, vol. 42, no. 8, pp. 1495–1512, 1995.
- [8] C. W. Helstrom, *Statistical Theory of Signal Detection*. New York: Pergamon, 1968.
- [9] H. L. Van Trees, *Detection, Estimation and Modulation Theory*, Part 1. New York: Wiley, 1968.
- [10] M. R. Bell, "Information theory and radar waveform designs," *IEEE Trans. Inform. Theory*, vol. 39, no. 5, pp. 1578–1597, 1993.
- [11] P. Narayan and D. L. Snyder, "Signal set design for band-limited memoryless multiple-access channels with soft decision demodulation," *IEEE Trans. Inform. Theory*, vol. 33, no. 4, pp. 539–556, 1987.
- [12] D. Slepian and H. O. Pollack, "Prolate spheroidal wave functions, Fourier analysis, and uncertainty—I," *Bell Syst. Tech. J.*, vol. 40, no. 1, pp. 43–63, 1961.
- [13] H. J. Landau and H. O. Pollack, "Prolate spheroidal wave functions, Fourier analysis, and uncertainty—II," *Bell Syst. Tech. J.*, vol. 40, no. 1, pp. 65–84, 1961.
- [14] ———, "Prolate spheroidal wave functions, Fourier analysis, and uncertainty—III: The dimension of the space of essentially time- and band-limited signals," *Bell Syst. Tech. J.*, vol. 41, no. 4, pp. 1295–1336, 1962.
- [15] A. W. Rihaczek, *Principles of High-Resolution Radar*. Monterey, CA: Peninsula, 1985.
- [16] J. R. Klauder, A. C. Price, S. Darlington, and W. J. Albersheim, "The theory and design of chirp radars," *Bell Syst. Tech. J.*, vol. 34, no. 4, pp. 745–808, 1960.
- [17] M. Abramowitz and I. Stegun, *Handbook of Mathematical Functions*. New York: Dover, 1970.
- [18] M. B. Pursley and H. F. A. Roefs, "Numerical evaluation of correlation parameters for optimal phases of binary shift-register sequences," *IEEE Trans. Commun.*, vol. 27, no. 10, pp. 1597–1604, 1979.



India. His current interests are in multiuser detection and multibeam imaging systems.



level and was promoted to Associate Scientist in 1988. He is currently an Associate Research Oceanographer at the Scripps Institution of Oceanography, Marine Physical Laboratory, University of California, San Diego which he joined in 1988. His research interests are in the areas of image reconstruction and restoration with a special emphasis on 3-D imaging systems. He is currently designing underwater optical and sonar imaging systems for ocean exploration.

Girish Chandran received the B.Sc. degree in physics from the University of Kerala, India, the M.E. degree in electrical communication engineering from the Indian Institute of Science, India, and the Ph.D. degree in electrical engineering at the University of California, San Diego, in 1985, 1989, and 1996, respectively.

He has worked on super-resolution spectrum estimation techniques and also on text-to-speech conversion systems for Indian languages at the Research and Development Electronics Laboratory, Bombay,

Jules S. Jaffe received the B.A. degree from the State University of New York, Buffalo, in physics, the M.S. degree in biomedical information science from the Georgia Institute of Technology, Atlanta, and the Ph.D. degree in biophysics from the University of California, Berkeley, in 1973, 1974 and 1982, respectively.

After spending several years working in industry as an Image-Processing Consultant, he joined the Woods Hole Oceanographic Institution as a Pew Memorial Fellow in 1984 at the Assistant Scientist